IOP Conference Series: Materials Science and Engineering

Comparison of behavior between hollow and composite K-joints under sustained loading and corrosion

To cite this article: S Saleh *et al* 2019 *IOP Conf. Ser.: Mater. Sci. Eng.* **513** 012039

IOP Conf. Series: Materials Science and Engineering **513** (2019) 012039 doi:10.1088/1757-899X/513/1/012039

Comparison of behavior between hollow and composite K-joints under sustained loading and corrosion

S Saleh[1*], M A Saqif[1] and F Ramiz[1]

[1] Department of Civil Engineering, University of Asia Pacific, Dhaka, Bangladesh

[*]Corresponding author: shameer.saleh@uap-bd.edu

Abstract. Concrete filled steel tubular (CFST) truss structures are widely being used in bridges and transmission towers all over the world. Design of connections is one of the most critical issues in truss structures; and it becomes even more complicated when corrosion causes loss of outer steel tube section. However, behavior of composite joints is among the least understood topics in structural engineering today. Previous attempts (numerical and experimental) to study the behavior of composite joints have focused mainly on the effect of sustained loading. But the widespread use of CFST structures in harsh, marine environment necessitates observing the performance of composite joints under corrosion alongside long-term loading. The aim of this paper therefore is to study the combined effect of chloride corrosion and sustained loading on circular composite K-joints through finite element analysis (FEA). The results thus obtained have been presented and verified against experimental observations of previous researchers. For a side by side comparison with composite K-joints, FEA has also been established for circular hollow section (CHS) K-joints. In addition to these, failure modes and load-deformation characteristics of both the composite and hollow K-joints have been thoroughly investigated under various practical loading cases and different corrosion scenario. From numerical analyses, it has been observed that corrosion in infilled chord leads to only 4% loss of joint strength whereas, corrosion of equal intensity in hollow braces decreases the joint capacity by 35%. Finally, joint strength and ductility have been predicted based on the full-range numerical analyses. Concrete infills have been found to enhance the joint strength by 2.5-3.0 times.

1. Introduction

For very long span bridges and tall transmission towers, lightweight hollow steel tubular sections are preferred over much heavier concrete sections. However, the inherent weakness of hollow steel sections to buckling and corrosion limits their use. It is apparent that both concrete and steel have inherent weaknesses that limit their applicability as structural members. Concrete is weak in tension and its behavior is affected by creep and shrinkage, whereas steel is prone to buckling and extremely susceptible to moisture. Steel-concrete composite structures utilize the strength of both the materials while significantly limiting their weaknesses. In concrete filled steel tubular (CFST) structures the infilled concrete prevents the outer steel tube from buckling while confinement of concrete by the outer tube results in higher ductility, greater section capacity and better fire and seismic resistance [1]. Consequently, improved performance and greater durability has led to the prevalence of CFST structures in marine environments (Figure 1). A fully rational understanding of the behavior of

IOP Conf. Series: Materials Science and Engineering **513** (2019) 012039 doi:10.1088/1757-899X/513/1/012039

composite joints is necessary to design CFST structures. Still the amount of research dedicated to studying the behavior of composite joints is fairly low as of today.

Several researchers in the past have studied the behavior of single composite members subjected to corrosive environment alongside sustained loading [2-4]. In those studies CFST members exhibited significantly better performance compared to CHS members. CFST members could resist a much higher load without inward buckling due to the presence of infill concrete. Also CFST members exhibited greater cross-sectional ductility and the members underwent far less load redistribution due to corrosion compared to CHS members. The behavior of the composite joints is greatly influenced by several cross sectional parameters such as steel to concrete ratio at composite chord (α), brace to chord diameter ratio (β), chord radius to thickness ratio (γ) and brace to chord thickness ratio (τ); which are affected during the corrosion process [5].

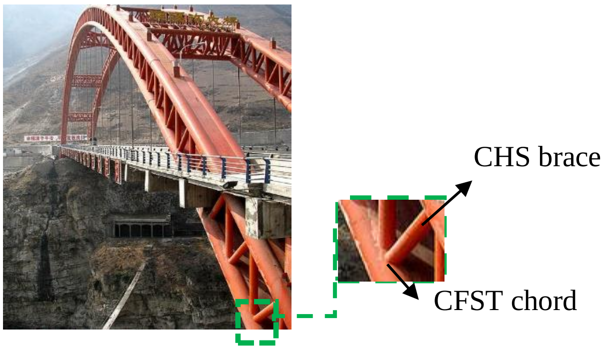

Figure 1. A bridge with circular CFST K-joints.

In this paper, the behavior of CFST K-joints has been investigated and their performance has been evaluated against CHS K-joints under sustained loading and various cases of chloride corrosion. A FEA model is established and verified against previously published experimental observations. The model is then utilized to perform mechanism analysis on both types of joints. Findings from full-range numerical analysis including load-deformation pattern and stress distribution have been presented and finally the joint strength is predicted.

2. Finite element analysis (FEA) model

Numerical models of CHS and CFST K-joints were developed using the finite element package ABAQUS to account for the combined effects of sustained loading and chloride corrosion. Dimensions and properties of K-joint samples in this research are adopted from experimental studies previously conducted [6]. The model is a further development of numerical behavior analysis of composite joints carried out in [7]. The combined effect of sustained loading and corrosion has been replicated by modifying the material properties in finite element model and by adopting 'Model change – Remove elements' interaction.

2.1. Development and configuration of K – joint

In the FEA model, two different types of material properties were selected for steel in joint tube and in end-plates. An elastic-plastic model with five distinct stages based on a previous study [8] was implemented to represent the steel behavior. For CFST K-joints, a damage-plasticity model was implemented to account for the core concrete plasticity behavior under both short-term and long-term loading with corrosion. The long-term stress-strain relationship was modified according to previous studies presented in [8] to reflect the time dependent factors of infilled concrete; such as creep and shrinkage. For the purpose of this paper, CHS-6 and CFST-6 with a brace and chord thickness of 6 and 10 mm respectively were chosen [6]. For CFST joint, the chord was infilled with concrete, whereas the braces were hollow.

The steel tube component of the joint has been modeled with 8-node linear 3-D solid element with reduced integration (C3D8R) to consider the effective section loss. Other components of the joint such as the infill concrete and end-plates are also simulated using the same element type. A proper meshing technique is crucial for the convergence and accuracy of FE simulation as composite K-joints are relatively complex in shape with particular local profiles. Structured meshing technique has been adopted where possible in order to achieve a proper element shape. However, the connection part of chord-brace tube was too complex to assign structured meshing due to irregularity of the plane. For the sake of simplicity, sweeping meshing technique was applied in the complicated connection area (Figure 2). A mesh convergence study was carried out to identify a suitable mesh size which provides tolerable simulation accuracy in reasonable computation time.

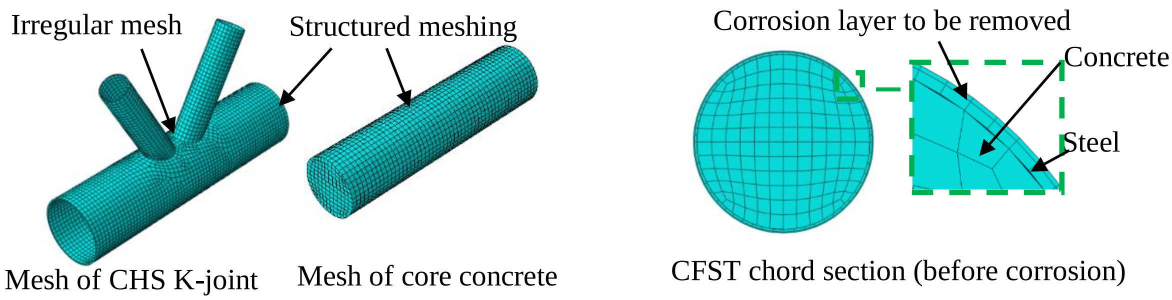

Figure 2. Meshing technique of CHS and CFST K-joint modeling.

2.2. Interface, boundary conditions and simulation of long-term loading with corrosion

The boundary conditions considered in this research were developed based on previously conducted studies [7, 9 and 10]. Axial static loading was applied in K-joints and the practical scenario was reflected by assessing three different boundary conditions, i.e., (1) compression load at chord, (2) compression load at brace and (3) tensile load at brace. Figure 3 illustrates the three distinct boundary conditions. Tie constraints were produced to simulate interaction between steel joint and end-plates. The contact interface between core concrete and steel tube in CFST joint was formed between two matching surfaces and by defining behavior along two orthogonal directions. These two surfaces are allowed to be separated from each other, whereas penetration into one another is not permissible. A 'Hard contact' model in normal direction and 'Coulomb friction model' in the tangential direction are adopted.

Corrosion is a fairly complex and uncertain natural phenomenon; and no numerical model has been able to replicate corrosion effects precisely. Therefore, current researches suggest considering corrosion at a constant rate which has a long-term uniform effect on outer steel of the joint tube [3, 4]. In this FEA model, the mass reduction and diameter loss of steel tube associated with corrosion has been simulated uniformly by a 'Model change – Remove elements' interaction. Corrosion is applied to

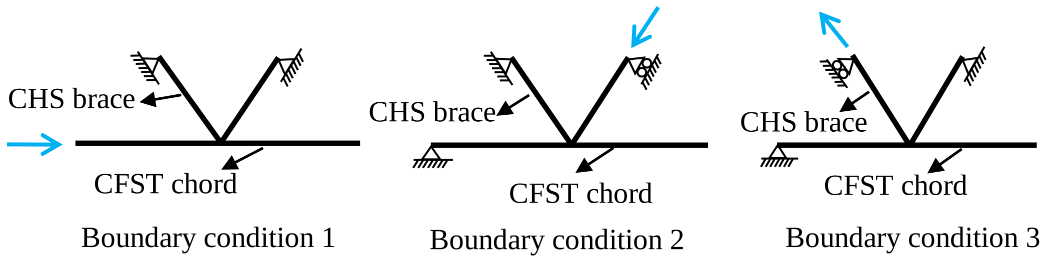

Figure 3. Typical boundary conditions considered for the study.

the model in four steps. First, partitioning the member affected by corrosion and defining corrosion set element; second, meshing of tube with several elements according to the corrosion thickness; third, creating a separate 'corrosion step' and selection of the corrosion region to deactivate in this step; and finally, adopting the new stress-strain relationship to represent steel-concrete confinement in corroded tubes (for CFST joints). Modified stress-strain relationship was applied by using the updated reduced dimensions of steel tubes under corrosion.

3. Verification of the FEA model

For verification of the results, two distinct approaches were used. One is comparing the load-displacement relation from numerical analysis with that of the experimental investigation carried out in [6]; the other is comparing the failure modes.

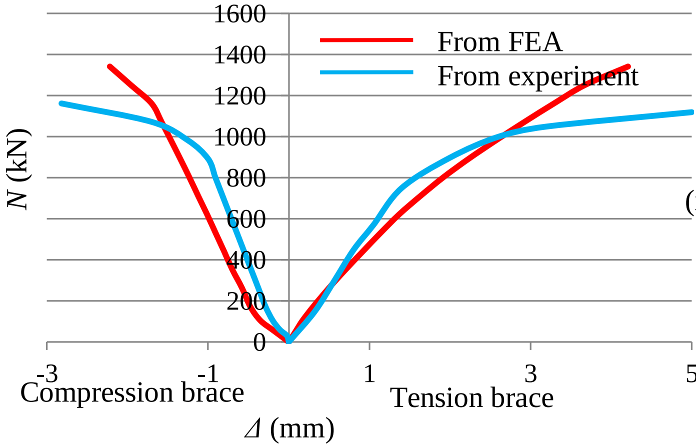

Figure 4. Comparison of the $N - \Delta$ relationship between experimental values and FEA.

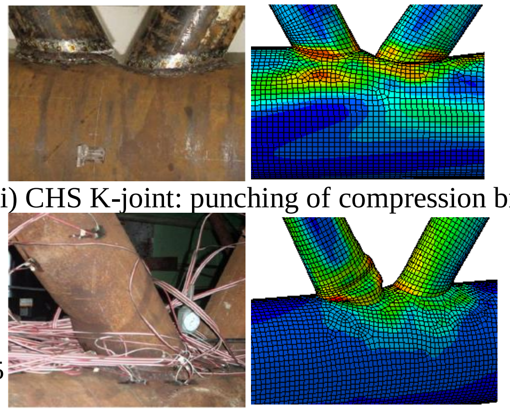

(i) CHS K-joint: punching of compression brace

(ii) CFST K-joint: outward local buckling in compression brace

Figure 5. Comparison between the experimental and numerically predicted failure modes.

It is apparent from Figure 4 that the results from FEA agree to the experimental values to a large extent. Chord stiffness has remained almost similar in FEA, but the ultimate load carrying capacity has exceeded the experimental value by almost ten percent. This can be attributed to ignoring the effect of welding at the brace-chord intersection in FEA. FEA has also depicted the failure patterns of CHS and CFST K-joints fairly accurately as can be seen from Figure 5. Failure of CHS K-joints occurs due to punching of the compression brace into the chord. However in CFST K-joints, infill concrete at the chord prevents punching failure. Outward local buckling of the compression brace along with bulging at the connection area is observed similar to the experimental observation. From the comparisons, it can be said with certainty that FE models are capable of reflecting the actual behavior of CHS and CFST K-joints. Hence further analysis run on the models considering sustained loading and chloride corrosion will be a near representation of the actual scenario.

4. Analytical behavior

4.1. Typical failure modes for CHS K-joints

Two failure modes are common with CHS K-joints (Figure 6). Since there is no infill concrete at the chord, the compression brace is likely to punch into the chord. At higher loads local buckling of chord takes place alongside punching of the compression brace.

4.1.1. Mode A: Punching in the chord

Punching of the compression brace occurs when moderate load is applied at the chord. Punching of brace is noticed at 20 mm chord displacement. Mises stress at the chord-brace connection is found to be around 384 MPa. Moderate chord plastification is noticed with corresponding Mises stress in the range of 260-320 MPa. No considerable local buckling is observed at the chord away from the connection.

4.1.2. Mode B: Punching in the chord combined with local buckling

This combined mode of failure was obtained when applied load at chord tube was significant. Noticeable plastic deformation of compression brace is observed along with severe punching, with maximum Mises stress of 497 MPa at critical brace region. Plastification of compression brace is

IOP Conf. Series: Materials Science and Engineering **513** (2019) 012039 doi:10.1088/1757-899X/513/1/012039

observed at stress level 280-350 MPa, while Mises stress at tension brace remains at moderate level (250-280 MPa). At time of compression brace failure, hollow chord tube fails due to inward buckling away from the connection. Buckling of the chord occurs at around 50 mm chord displacement; and stress at chord region remains at moderate level (270-320 MPa).

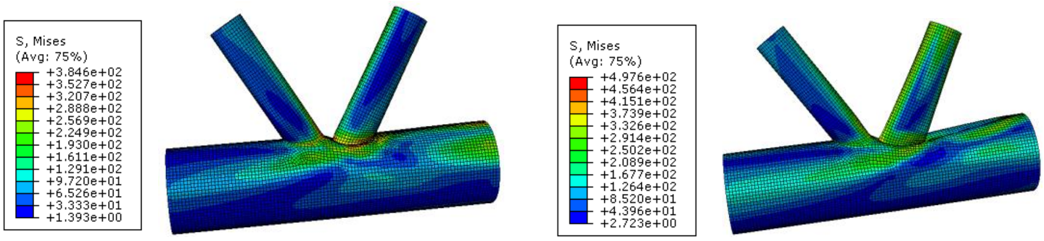

(a) Punching in the chord (b) Punching in the chord combined with local buckling

Figure 6. Typical failure modes for CHS K-joints.

4.2. Typical failure modes for CFST K-joints

Presence of infill concrete in the chord makes CFST K-joints bear higher load than CHS K-joints as compression brace can no longer punch into the chord. Depending on different boundary condition, three types of failures have been observed.

4.2.1. Mode A: Plastification of chord

When moderate amount of load is applied at the chord, this failure mode is noticed (Figure 7). A significant portion of the chord undergoes plastification at the chord-brace intersection area as the Mises stress stands to be 431 MPa. Inside the chord, the outer region of the core concrete receives the maximum stress (around 58 MPa) on the areas where chord plastification is prominent. At the braces the Mises stress stays in the 280-340 MPa range and with no observable local buckling.

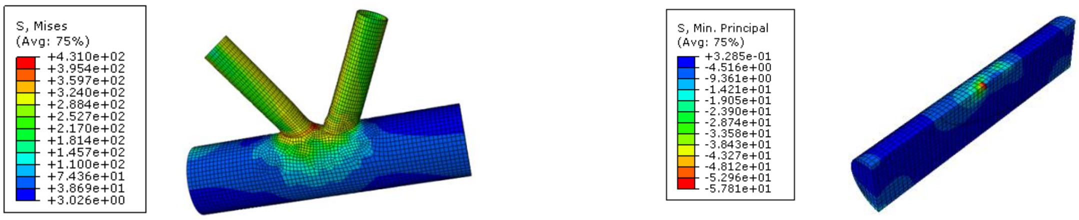

(a) Overview of the joint (b) Inner concrete (cut view)

Figure 7. Chord plastification of CFST K-joints.

The infill concrete in the chord increases the resistance of the CFST K-joint since the core concrete prevents the inward buckling of the compression braces, a phenomenon very common to CHS joints.

4.2.2. Mode B: Chord plastification combined with local buckling of the brace

This failure mode can be observed when a large load is applied at the chord end (Figure 8). At the onset of failure, the chord tube at the connection region reaches plastic state, and then noticeable local buckling of the compression brace takes place.

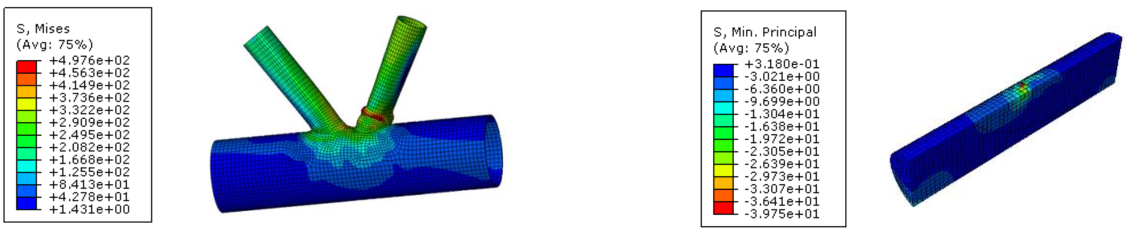

(a) Overview of the joint (b) Inner concrete (cut view)

Figure 8. Chord plastification and local buckling of brace of CFST K-joints.

High stress concentration is found at the region of local buckling as the hollow brace section fails at Mises stress of 497 MPa. Tension brace and chord remain moderately stressed (310-350 MPa) when the joint fails. Only the outer region of core concrete receives stress at the joint (nearly 40 MPa), inner regions remain almost unstressed.

4.2.3. Mode C: Premature local buckling of the brace

Initially a small region in the tension brace enters the plastic stage in this mode. However, as loading continues, localized stresses accumulating in the compression brace lead to yielding in the connection region. Unlike the first two failure modes, here the entire compression brace fails in local buckling as large plastic deformation sets in while the chord remains elastic (Figure 9). Mises stress at the critical sections of the brace tube reaches 493 MPa but the stresses at the intersection stays within the elastic limit. At the critical intersection region, core concrete is stressed up to around 55 MPa. Stress at the concrete surface in this mode is similar to Mode A and approximately 38% higher than Mode B.

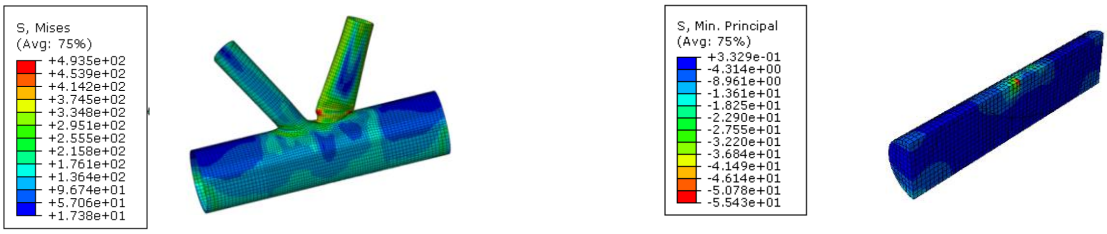

(a) Overview of the joint (b) Inner concrete (cut view)

Figure 9. Premature local buckling of brace of CFST K-joints.

Failure modes B and C are quite similar except for chord plastification in the former one. Compared to CHS joints, CFST joints are stronger since punching of compression brace into the chord is prevented by the infilled concrete. For both CHS and CFST joints, compression brace is found to be the critical element.

5. Full range analysis

5.1. Typical full-range load-displacement relationship

Full-range analyses of CHS and CFST K-joints have been performed using FEA models. Figure 10 demonstrates the typical load *(N)* versus displacement *(Δ)* relationships of CFST K-joints under short-term loading and long-term loading with corrosion.

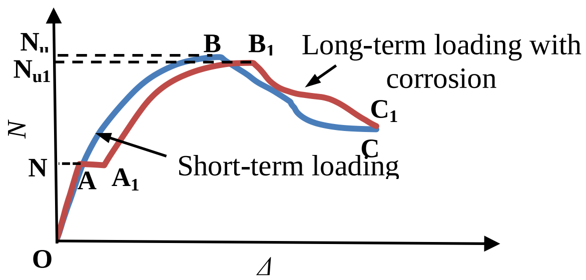

Figure 10. Typical *N- Δ* relationship of CFST K-joints before and after corrosion.

Curve O-A-B-C shows the short-term loading condition before corrosion has taken place. It is apparent from the curve that CFST K-joints exhibit excellent ductile behavior as the joint fails long after attaining its ultimate capacity (N_u). Curve O-A-A_1-B_1-C_1 displays the *N-Δ* relationship of CFST K-joints under long-term loading and corrosion. This curve has four distinct parts. At elastic stage (O-A), the response is elastic up to application of the load N_1. At corrosion stage (A-A_1), the load N_1 is

IOP Conf. Series: Materials Science and Engineering **513** (2019) 012039 doi:10.1088/1757-899X/513/1/012039

kept constant and uniform corrosion is applied, thereby creating the combined effect of sustained loading and corrosion. Corrosion is applied in the form of loss of thickness in outer steel tube which results in deformation growing up to A_1. Time dependent behaviors of concrete, e.g. creep and shrinkage also manifest at this stage. Corrosion not only gives rise to stress redistribution between steel and concrete but it also adversely affects the confinement of core concrete. The following elastic-plastic stage (A_1-B_1) is marked by continued loading up to ultimate joint capacity (N_{u1}). Significant loss of stiffness and ultimate strength is prominent when corrosion takes place alongside long-term loading. At descend stage (B_1-C_1), deformation keeps increasing while the axial load decreases. The declining limb of the curve reflects the degree of corrosion and the extent of composite action in the CFST chord. A noteworthy finding is that, effect of corrosion on the declining stage is much less severe than the effect of composite action. Overall performance of CFST K-joints is significantly better under long-term loading combined with corrosion compared to CHS K-joints.

5.2. Effects of different corrosion patterns

Full-range analysis of CHS K-joints in Figure 11(a) shows significant reduction of joint capacities as corrosion occurs. A 13% reduction in strength is noticed for a 30% thickness loss due to corrosion either in chord or brace. When corrosion occurs throughout the joint, the joint capacity decreases even further. For a thickness loss of 30% in steel tubes, joint capacity reduction is noticed as 26%. From load-displacement relationship in Figure 11(b) of CFST K-joints, it is evident that corrosion in chord has an insignificant effect on the performance of the joints in terms of ductility and ultimate strength. When the chord thickness decreases by as much as 30%, the corresponding loss of joint capacity is a mere 4%. The infilled concrete improves the resistance of the chord; and thereby prevents premature local buckling, leading to a stronger and more ductile joint behavior. As opposed to corrosion in chord, the joint capacity is severely impaired when brace member is corroded. For a brace thickness loss of 30% due to chloride corrosion, joint capacity reduction of nearly 35% has been observed. Besides reduction in strength, brace corrosion also decreases the ductility of the joints. The chord displacement at ultimate load observed for chord corrosion is 35mm which falls drastically to just 18mm when brace is exposed to corrosion.

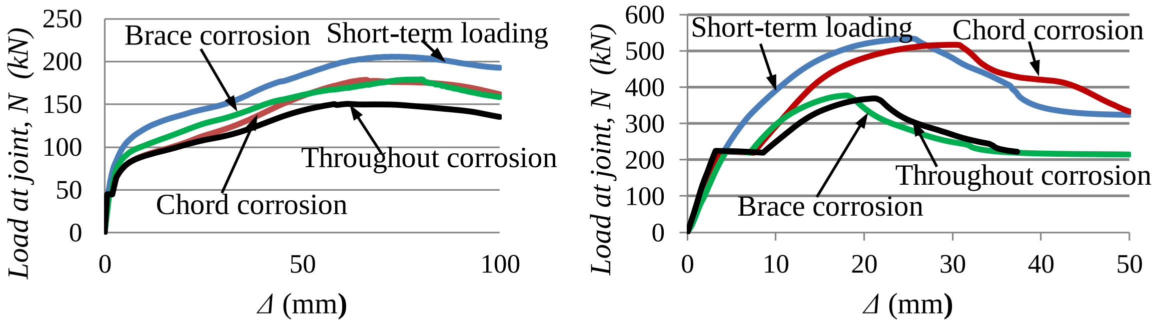

(a) CHS K-joints (b) CFST K-joints

Figure 11. *N*-*Δ* relationship of K-joints for different corrosion conditions.

Ultimate load at failure for different boundary conditions and corrosion patterns has been presented in Table 1. It can be seen that infilled concrete improves joint capacity significantly. CFST joint strength is found to be around 250 – 300% compared to CHS joints.

Table 1. Comparison of CHS and CFST joint capacities under various corrosion conditions.

Corrosion condition	Load at chord (kN)		Load at compression brace (kN)		Load at tension brace (kN)	
	CHS 6	CFST 6	CHS 6	CFST 6	CHS 6	CFST 6
Before corrosion	205	533	223	594	259	522
Chord only corrosion	178	517	212	583	215	498
Brace only corrosion	178	376	210	397	207	369
Throughout corrosion	150	368	159	393	198	357

As corrosion sets in, joint capacities reduce regardless of the boundary condition. Corrosion throughout the joint has almost the same effect as corrosion only in the braces of CFST joints. From the full-range analysis, it can be concluded that regardless of boundary condition and corrosion case, the hollow compression brace is the critical member in K-joints.

6. Conclusion

Based on the research conducted in development of this paper, following conclusions can be drawn:
(1) FEA of composite joints can be used to verify experimental observations of previous researchers, as the results obtained from ABAQUS agree to the experimental investigations to a large degree.
(2) Two distinct failure modes for CHS and three for CFST K-joints have been observed for long-term loading with corrosion. Hollow compression brace has been identified as the critical member in the connection regardless of the boundary condition.
(3) From full-range analysis, it is apparent that corrosion of chord has only moderate influence on the behavior of the joints. However, corrosion on the braces affects the joint performance significantly.
(4) Punching shear is the predominant mode of failure in CHS joints. Punching starts at low displacement and although load carried by the chord keeps increasing during FEA, joint had already failed in punching, exhibiting poor ductility.
(5) Load carrying capacity of CFST K-joints starts to decrease when interaction between steel and concrete is affected, i.e. high degree of composite action leads to higher joint strength.
(6) Infill concrete does not significantly contribute in bearing the loads applied to CFST K-joints. Rather its function is to delay the yield propagation and avoid premature buckling. Resistance and ductility of the joints improve greatly when concrete infills are used inside hollow steel tubes.

References

[1] Han L H, Li W and Bjorhovde R 2014 Developments and advanced applications of concrete-filled steel tubular (CFST) structures: members. *Journal of Constructional Steel Research.* **100**(1): 211-28.
[2] Han L H, Hou C and Wang Q L 2012 Square concrete filled steel tubular (CFST) members under loading and chloride corrosion: Experiments. *Journal of Constructional Steel Research.* **71**: 11-25.
[3] Hou C, Han L H and Zhao X L 2013 Full-range analysis on square CFST stub columns and beams under loading and chloride corrosion. *Thin-Walled Structures.* **68**: 50-64.
[4] Han L H, Hua Y X, Hou C and Wang Q L 2017 Circular concrete-filled steel tubes subjected to coupled tension and chloride corrosion. *Journal of Structural Engineering.* **143**(10) :04017134-1.
[5] Wardenier J, Packer J A, Zhao X L and Vegte G J 2010 *Hollow sections in structural applications, Delft: Bouwen met Staal*.
[6] Huang W, Fenu L, Chen B and Briseghella B 2015 Experimental study on K-joints of concrete-filled steel tubular truss structures. *Journal of Constructional Steel Research.* **107**:182-93.

[7] Saleh S, Hou C, Han L H and Hua Y X 2018 Numerical behavior of composite K-joints subjected to combined loading and corrosive environment. *12th International Conference on Advances in Steel-Concrete Composite Structures ASCCS 2018* (Valencia-Spain).

[8] Han L H, Tao Z and Liu W 2004 Effects of sustained load on concrete-filled hollow structural steel columns. *Journal of Structural Engineering, ASCE*. **130**(9): 1392–404.

[9] Song Q Y and Han L H 2010 FE analysis of composite tubular K-joints subjected to static loading. *Tubular Structures XIII – Young (ed);* (Hong Kong: The University of Hong Kong) ISBN 978-0-415-58473-9.

[10] Hou C, Han L H and Mu T M 2017 Behaviour of CFDST chord to CHS brace composite K-joints: Experiments. *Journal of Constructional Steel Research*. **135**:97-109.